Diclofenac prodrugs nanoparticles: an alternative and efficient treatment for rheumatoid arthritis?

Saadat Hussain, Mujeeb Ur-Rehman, Aqsa Arif, Catherine Cailleau, Cynthia Gillet, Rudaba Saleem, Hira Noor, Farwa Naqvi, Almas Jabeen, M. Iqbal Choudhary, et al.

Diclofenac prodrugs nanoparticles: an alternative and efficient treatment for rheumatoid arthritis?

Saadat Hussain[a], Mujeeb Ur Rehman [a*], Aqsa Arif[a], Catherine Cailleau[b], Cynthia Gillet[c], Rudaba Saleem[a], Hira Noor[d], Farwa Naqvi[d], Almas Jabeen[d], Atta-ur-Rahman[a,d], M. Iqbal Choudhary[a,d], Elias Fattal[b], Nicolas Tsapis[b*].

[a]L. E. J. Nanotechnology Center, H. E. J. Research Institute of Chemistry, International Center for Chemical and Biological Sciences, University of Karachi, Karachi-75270, Pakistan.
[b]Université Paris-Saclay, CNRS, Institut Galien Paris-Saclay, 91400 Orsay, France.
[c]Université Paris-Saclay, CEA, CNRS, Institute for Integrative Biology of the Cell (I2BC), 91198, Gif-sur-Yvette, France.
[d]Dr. Panjwani Center for Molecular Medicine and Drug Research, International Center for Chemical and Biological Sciences, University of Karachi, Karachi-75270, Pakistan.

***Corresponding authors:**
Mujeeb-ur-Rehman (mbtk.chem@gmail.com),
Nicolas Tsapis (nicolas.tsapis@universite-paris-saclay.fr)

Key words: Diclofenac, Prodrug, Nanoparticle, Inflammation, Rheumatoid arthritis

Graphical abstract

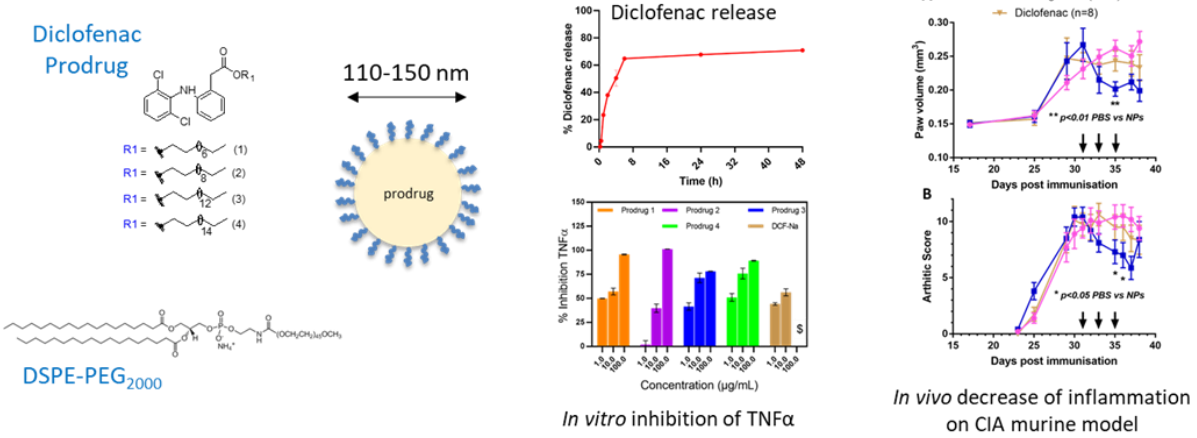

In vitro inhibition of TNFα

In vivo decrease of inflammation on CIA murine model

Abstract

We have synthesized new lipidic prodrugs of diclofenac by grafting aliphatic chains (C10, C12, C16 and C18) to diclofenac through an ester bond. Their molecular formulas were confirmed through HR-MS and the formation of ester bond by FTIR and NMR spectroscopy. Nanoparticles of the different prodrugs were successfully formulated using emulsion evaporation method and DSPE-PEG_{2000} as the only excipient. All nanoparticles were spherical and had a size between 110 and 150 nm, PdI ≤ 0.2 and negative Zeta potential values from -30 to -50 mV. In addition, they were stable upon storage at 4°C up to 30-35 days. The encapsulation efficiency of the prodrug was above 90% independently of the aliphatic chain length grafted. Nanoparticles did not induce any toxicity on LPS-activated THP1 cells up to a concentration of 100 µg/mL (equivalent diclofenac) whereas diclofenac sodium salt IC_{50} was around 20 µg/mL. Following incubation of nanoparticles with LPS-activated THP1 cells, a dose dependent inhibition of TNF-α was observed comparable to standard diclofenac sodium. Based on *in vitro* studies representative nanoparticles, Prodrug **3** NPs (C16 aliphatic chain) were selected for further *in vitro* and *in vivo* studies. Upon incubation in murine plasma, Prodrug **3** NPs underwent an enzymatic cleavage and almost 70 % of diclofenac was released from nanoparticles in 8 hours. *In vivo* studies on a collagen induced arthritis murine model showed contrasted results: on one hand Prodrug 3 NPs led to a significant decrease of arthritis score and of paw volume compared to PBS after the second injection, on the other hand the third injection induced an important hepatic toxicity with the death of half of the mice from the NP group. To promote the reduction of inflammation while avoiding hepatic toxicity using NPs would require to precisely study the No Observable Adverse Effect Level and the schedule of administration in the future.

1. Introduction

Rheumatoid arthritis (RA) is a chronic autoimmune disease where stiffness, swelling and destruction of joints occurs. The worst impacts of RA include the possibility of disability, a 10-year decrease in life expectancy, increased angiogenesis, and a lower quality of life. It affects 0.3 to 2.6% of population (Alamanos et al., 2006; Andrianakos et al., 2006; Carmona et al., 2002; Jacobs et al., 2011; Langley et al., 2011; Myasoedova et al., 2020; Neovius et al., 2011). The exact origin of RA is unknown but certain environmental and genetic factors may lead to this pathology (Mellado et al., 2015). Currently treatments of RA rely on glucocorticoids, disease-modifying anti-rheumatic drugs (DMARDs) (e.g. methotrexate), targeted DMARDs (e.g. Janus kinase inhibitors) biological DMARDs among which tumor necrosis factor TNF-α inhibitors or even non-steroidal anti-inflammatory drugs (Chatzidionysiou et al., 2017). Once administered, the drugs distribute at the pathological sites but also in healthy tissues, leading to unwanted side-effects. Indeed, drugs with undesired pharmacokinetic parameters, short half-life, rapid elimination, and large volume of biodistribution lacks efficacy due to poor accumulation of the drug in the desired inflamed sites. To better target inflamed sites by taking advantage of the specific physiopathology of inflamed tissues such as their enhanced vascular permeability, nanomedicines can be considered. By passive diffusion nanomedicines can accumulate in inflamed joints and improve anti-inflammatory activity while avoiding high doses and thus side- effects (Dolati et al., 2016; Lorscheider et al., 2019b; Ozbakir et al., 2014). Many nanomedicines works on RA focused on the encapsulation and delivery of glucocorticoids while less attention is given to NSAIDs (Al-Lawati et al., 2019).

In this study, we have synthesized new prodrugs of a well-known NSAID, Diclofenac by grafting alkyl chains of different lengths (from C10, C12, C16 or C18) to Diclofenac by esterification. The four prodrugs synthesized and their corresponding spectra are reported for the first time in the literature. Prodrugs were then formulated into nanoparticles by sole addition of DSPE-PEG2000 as an excipient using a simple emulsion-evaporation process recently patented for glucocorticoids (Lorscheider et al., 2019b). This process was shown to yield higher drug loading for glucocorticoids (> 50%) than physical encapsulation into liposomes or polymer nanoparticles (Lorscheider et al., 2019a). To the best of our knowledge, testing this strategy with a NSAID such as Diclofenac was never reported and would shed light on the ability to extend the process to other drugs than glucocorticoids. Nanoparticles were physico-chemically characterized by dynamic light scattering, zeta potential measurements, and electronic microscopies. UPLC was employed to quantify prodrug encapsulation efficiency. Alamar blue assay was performed to analyze *in vitro* cytotoxicity on THP-1 cell line. The anti- inflammatory activity of nanoparticles was tested by ELISA on LPS activated THP-1 cells, Finally, nanoparticles obtained with C16 prodrug were injected in a model of collagen induced arthritic mice, to evaluate their anti-inflammatory activity in vivo.

2. Material and methods

2.1 Materials

Diclofenac Sodium, 1-(3-Dimethylaminopropyl)-3-ethylcarbodiimide hydrochloride (EDC HCl), Dimethylamine pyridine (DMAP), Dimethylformamide (DMF), D-Glucose, 4-(2-hydroxyethyl)-1-piperazineethanesulfonic acid (HEPES) and RPMI-1640 were bought form Sigma Aldrich, USA. Decyl alcohol, lauryl alcohol, cetyl alcohol and stearyl alcohol were bought form Daejung Reagent Chemicals, Korea. Likewise, Ethanol from J.T. Baker, USA, Dichloromethane, Chloroform from VWR Chemicals, France and FBS (PAA Laboratories, Austria), 1,2-distearoyl-sn-glycero-3-phosphoethanolamine-N-[amino(polyethylene glycol)-2000] (DSPE-PEG_{2000}, 880120P of Avanti Polar Lipids.Inc.), 2- mercaptoethanol (Biomedicals, France); Sodium Pyruvate (Gibco, USA), PMA and BSA(Biomedicals, France) Lipopolysaccharide B of E. coli 0111:B4 (LPS) (DIFCO, USA), flat bottom 96-well tissue culture plates (Corning, USA), Human TNFα-DuoSet ELISA Kit (R&D Systems, USA), clear flat bottom 96-well microplates (Minneapolis, USA), PBS tablets (Bio globe, USA), and Tween 20 (Minneapolis, USA).

2.2 Diclofenac Prodrugs Chemical Synthesis

Diclofenac acid (0.25 mM, 74.03 mg) was first dissolved in dichloromethane (DCM) (10 mL) in a round-bottom flask (250 mL) under magnetic stirring. After adding 30.54 mg (0.25 mM) DMAP and ice-cooling the mixture to 0°C when it became clear, 51.7 mg (0.275 mM) EDC was added (Tsakos et al., 2015). The desired fatty alcohol reagent (0.5 mM) (1-decanol 98.18 µL, 1-dodecanol 112 µL, cetyl alcohol 121.22 mg, and stearyl alcohol 135.24 mg, respectively, for the desired reaction) was added to this reaction mixture. Reaction was left for completion (24 h). Thin layer chromatography (TLC) confirmed completion of reaction followed by workup using brine water and three times extraction with DCM. Utilizing column chromatography and the DCM: Hexane (30:70) solvent system, the product was purified. The structural elucidation of prodrugs was accomplished using the Advance Bruker 500MHz NMR, EI-MS/HR-EIMS, and FTIR Bruker Vector 22 techniques.

The prodrugs synthesized are Diclofenac decyl ester (1) EI-MS: m/z 435.3 [M]+, 437.3, [M+2] +, Diclofenac Lauryl Ester (2) EI-MS: m/z 465.2 [M+2] +, 463.2 [M]+, Diclofenac hexadecyl ester (3) EI-MS: m/z519.3 [M]+, 521.3 [M+2] +, Diclofenac octadecyl ester (4) EI-MS: m/z 547.3 [M]+, 549.3 [M+2] +, Diclofenac ethyl ester (5) EI-MS: m/z 423.1 [M]+ 325.1 [M+2] + and Diclofenac butyl ester (6) EI-MS: m/z 353.1 [M+2] +, 351.1 [M]+. See in Supporting Information S1.

2.3 Formulation of Diclofenac prodrugs as nanoparticles (NPs)

Nanoparticles were prepared via an emulsion-evaporation process. DSPE-PEG_{2000} is used as excipient to avoid Diclofenac recrystallization and ensure formation of stable nanoparticles with maximal encapsulation of prodrugs (Gaudin et al., 2014; Leng et al., 2014; Lorscheider et al., 2019a; Maksimenko et al., 2014; Quan et al., 2014). The

lipophilic prodrug(s) (25 mg) and DSPE-PEG_{2000} (12.5 mg) were dissolved in 1 mL chloroform at a 2:1 prodrug to DSPE-PEG_{2000} ratio (w:w). The prodrug and DSPE-PEG_{2000} mixture was injected into 5 mL of deionized water that pre-chilled (4 °C) and then vortexed for 30 s to form a crude emulsion. Following that, 3 minutes of probe sonication (Sonics, Ultrasonic processor, Vibra-Cell, model: VCX130PB, USA) was conducted. A rotary evaporator with a bath temperature of 60 °C was then used to evaporate the organic solvent, at a pressure of 300 mbar, initially for the first 30 minutes, and then a pressure of 200 mbar for the following 30 minutes. The final suspension volume was then completed to 5 mL and kept at room temperature and 4 °C until further examination.

2.4. Dynamic Light Scattering (DLS)

Using a NanoZetaSizer ZSP (Malvern) and a He-Ne laser of 4 mW as light source operating at 633 nm, DLS measurements were carried out after dilution 20 times in deionized water. The sample was allowed to equilibrate for 60 s at 25°C for all measurements, which were done in automatic mode. After dilution (20 times) in a 1 mM NaCl solution, NPs zeta potential was assessed using disposable folded capillary cells (DTS1070).

2.5. Scanning Electron Microscopy (SEM)

The samples were analyzed by scanning electron microscopy (Apreo 2 C, Lovac, ThermoScientific) at ICCBS, University of Karachi. Liquid samples were deposited onto a carbon tape surface then dried and coated with a thin gold layer using a sputter coater.

2.6. Transmission Electron Microscopy (TEM)

Prodrug 1-4 NPs were examined using a MET JEOL 1400 TEM (80KV) at I2BC (CNRS, Gif-sur-Yvette, France). 5 µL of a nanoparticle suspension were deposited for 40 s on copper grids coated with 400 mesh formwar and blotted of using Whatman filter paper. Samples were then negatively stained with uranyl acetate (2% w/w) and blotted again. Pictures were taken using an Orios Camera.

2.7. Determination of encapsulation efficiency (EE) of prodrugs in NPs

To distinguish between non-encapsulated prodrugs and prodrugs in nanoparticles, ultracentrifugation was performed using Sorvall WX+ (ThermoFisher Scientific) ultracentrifuge at 35000 rpm for 4 hours at 4 °C. Following separation of the supernatant and the pellet, the supernatant was freeze-dried before analysis. 500 µL of nanoparticle suspension was also freeze-dried for quantification. UPLC (Agilent Technologies) connected to a PDA detector was used to quantify prodrug in supernatant and NPs. PDA detection was carried out at a wavelength of 281 nm. The stationary phase used, ECLIPSE XDB-C8 (3 x 30 mm, 1.8 µm), was eluted for 5 minutes at a flow rate of 0.5 mL/min with varied polarity for each prodrug as shown below in Table-1 in supporting file S1. Acetonitrile (0.1% trifluoracetic acid) and H2O (0.1% trifluoracetic

acid) were employed as the mobile phase. To provide an adequate concentration within the calibration curve, the freeze dried supernatant and nanoformulations were dissolved in 100% ACN. Each sample was injected in a volume of 3 µL, and the run time was set to 5 minutes. Concentrations between 0.1 and 750 µg/mL were prepared to create calibration curves for quantification, and a standard calibration curve was created for each prodrug followed a linear model, Prodrug 1 (y= 5.5757x 1.7046 and R2= 0.9994), Prodrug 2 (y= 5.8462x – 14.635 and R2= 0.9995), Prodrug 3 (y = 5.0521x + 6.9091 and R2 = 0.9999) and Prodrug 4 (y= 3.9727x + 3.8145 and R2= 0.9996).

2.8. *In vitro* drug release in mice plasma

1900 µL of murine plasma were taken in an Eppendorf tube, 100 µL of prodrug **3** NPs were added and incubated at 37 °C upon gentle agitation for different times up to 48 h (Lorscheider et al., 2019b). 200 µL of sample was taken out from the Eppendorf at different interval of time till 48 h. The sample was then extracted with acetonitrile (800 µL) containing diclofenac ethyl ester as internal standard to determine the extraction efficiency of the system. The sample was vortex vigorously for 3 minutes to precipitate out enzymes/proteins present in plasma. Then, centrifugation was performed at 14500 rpm for 10 min. The supernatant organic phase was collected and Diclofenac was immediately quantified by UPLC connected to PDA detector to avoid further degradation of the prodrug. PDA detection was carried out at a wavelength of 281 nm. Acetonitrile and H_2O, used as the gradient-based mobile phase, were eluted from the employed column, ECLIPSE XDB-C8 (3 x 30mm, 1.8µm), for 14 minutes at a flow rate of 0.4 mL/min. Calibration curve was established for Diclofenac from concentration range of 1 µg to 100 µg with regression curve value of 0.9982, y= 6.5014 + 12.911. Retention times were 1.2 min for diclofenac and 5.9 min for prodrug **3**.

2.9. NPs toxicity on cells

The Alamar blue assay was used to determine the cytotoxicity of NPs and parent drug on the THP-1 cell line. Cell culture medium used was 10% RPMI and cell providers were ECACC. Cells were plated at a seeding density of 1x105 cells per milliliter. The cells were exposed to a 3 concentrations of parent drug or NPs as equivalent parent drug (1, 10, and 100 µg/mL) for 24 hours. After adding 10 µL of Alamar blue dye to each well, the plate was incubated for an additional 24 hours. Readings were taken in a spectrophotometer at wavelengths of 570 nm and 600 nm.

2.10. In Vitro Studies on against prominent proinflammatory cytokines

As different studies have been carried out in literature for analysis of in vitro efficacy of diclofenac and its nanoparticles (Al-Amin et al., 2013; Assali et al., 2021, 2018), the THP-1 cell line was used and the secretion of pro-inflammatory TNFα cytokine quantified. In addition to 10% fetal bovine serum (FBS), L-glutamine, 50 µmol, 2 mM/L mercaptoethanol, 5.5 mmol glucose, and HEPES (4-(2-hydroxyethyl)-1-piperazine-

ethane-sulfonic acid) 10 mM/L, THP-1 cells were grown in RPMI-1640. Cells were collected and plated in a 24-well cell culture plate at a density of 2.5 x10^5 cells/mL once they had reached 70% confluence. 20 ng/mL phorbol myristate acetate (PMA) was added to the cells to differentiate them, and they were then incubated overnight at 37 °C in a 5% CO2 incubator. After incubation, 50 ng/mL of E. coli Lipopolysaccharide (LPS) was added to the cells to activate them, followed by treatment with free diclofenac or prodrugs NPs at equivalent diclofenac concentrations of 1, 10, and 100 µg/mL for 24 hours at 37 °C in an incubator with 5% CO2. The cell supernatant was collected in Eppendorf tubes and kept at -20°C. The manufacturer's recommendations were followed while utilizing a human ELISA kit for TNFα. Negative and positive control were detailed as C= non treated cells and C+P+L= cells treated with PMA and LPS, respectively. Cytokine inhibition percentage was calculated as [100-(conc. of sample/conc. of C+P+L)] x100.

2.11. *In Vivo* Studies on Collagen-induced arthritis murine model

In vivo experimental procedures using DBA/1OlaHsd mice were approved by the ethical committee No 026 and the French ministry of education and research (Accepted protocol No 2842-2015110914248481_v5). Male DBA/1OlaHsd mice, 6-8 weeks old, 15-22g, were purchased from Envigo (Gannat, France) and let for one week after the reception for adaptation before starting the experiments. The mice were housed with access to water and food ad libitum and maintained at a constant temperature (19-22°C) and relative humidity (45-65%).

The collagen-induced arthritis model was performed as follows. In brief, complete Freund's adjuvant and chicken type II collagen dissolved in diluted acetic acid were mixed at a 1:1 ratio (v:v). This mixture was emulsified into a creamy emulsion using a tissue homogenizer. On day 0, after anesthesia with isoflurane, mice were injected with 50 µL of the emulsion at the tail base intradermally. A second injection (boost) was performed on day 21. After the second injection, mice were monitored every 2 days, including weight, hind paw volume, and arthritis scoring. The scoring criteria are described below.

0 = normal, 1 = one or two digits inflamed (red and thickened), 2 = all of the digits inflamed (red and thickened) and moderate swelling of the foot, 3 = redness and increased swelling of ankle and foot, 4 = severe swelling of whole paw and digits. The hind paw volume was measured using a plethysmometer (Harvard Apparatus).

On day 30, most mice showed apparent symptoms of arthritis. Mice were assigned to 3 groups to equalize the sum of the scores of each group. On day 31, the mice were injected into the iliac plexus vein under isoflurane anesthesia with either 200 µL of PBS, 200 µL of Diclofenac sodium salt (10mg/kg), 200 µL of Diclofenac Prodrug **3** NPs (10mg/kg equivalent Diclofenac). Injections were repeated on days 33 and 35.

2.12 Statistical analysis

Statistical analysis was performed using 2-way ANOVA and Dunnet post comparison tests using GraphPad Prism software.

3 Results and Discussion

3.1 Chemical Synthesis and Structural Characterization of Prodrugs of Diclofenac

All of the prodrugs of Diclofenac synthesized as detailed in Scheme 1 were analyzed by NMR, EI-MS/HR-EIMS and FTIR techniques. The molecular formula of the prodrugs (**1**-**4**) was validated by HR-MS. Additionally, FTIR was used to establish the formation of the ester bond. The results were compared to those obtained for the Diclofenac (Figure-1).

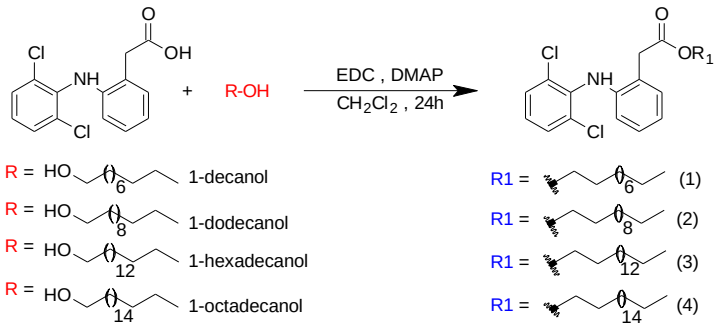

Scheme 1: Diclofenac prodrugs (**1**-**4**) with ester linkage of different aliphatic chain lengths.

Prodrug 1: Decyl 2-(2-((2,6-dichlorophenyl) amino) phenyl) acetate (1)

The molecular formula $C_{24}H_{31}Cl_2NO_2$ was determined from the EIMS of prodrug **1** and the HREI-MS, which revealed M+ at *m/z* 435.1732 with Δ ppm -1.4 and suggested a decreased double bond value of 9 (Calculated Molecular Weight (MW) 435.1725). Sharp bands may be seen in the IR spectrum at 3454 cm $^{-1}$ (NH) and at 2926.5-2854.1 cm $^{-1}$ typical signature of the C-H of grafted aliphatic carbon chain. Moreover, a robust band at 1719 cm $^{-1}$ (COOR) indicating the presence of ester carbonyl group. The compound's ^{1}H, and ^{13}C-NMR chemical shifts revealed characteristic peaks for 24 carbons, including 10 aliphatic carbons, one methyl carbon [δ_H 0.85 (t) $J_{(9', 10')}$ = 8.8Hz H-10 ’] and one oxygenated methyl [δ_H 4.11 t, $J_{(2', 1')}$ = 8.5Hz, 2H, CH_2-OCO H-1’]= 8.5Hz, 2H, CH_2-OCO H-1]. The prodrug 1's detailed spectroscopic data is given in **Supporting Information S1**.

Prodrug 2: Dodecyl 2-(2-((2,6-dichlorophenyl) amino) phenyl) acetate (2)

The molecular formula $C_{26}H_{35}Cl_2NO_2$ was determined from the EIMS of prodrug **2** and the HREI-MS, which revealed M+ at *m/z* 463.2045 with Δ ppm -0.8 and suggested a decreased double bond value of 9 (Calculated Molecular Weight (MW) 463.2037). Sharp bands may be seen in the IR spectrum at 3316 cm $^{-1}$ (NH) and 2959.7-2952.2 cm $^{-1}$ (aliphatic carbons). Moreover, a robust band at 1720.4 cm $^{-1}$ (COOR). The compound's ^{1}H and ^{13}C-NMR chemical shifts revealed characteristic peaks for 24 carbons, including 12 aliphatic carbons, one methyl carbon [δ_H 0.85 (t) $J_{(11', 12')}$ = 8.8Hz H-12 ’]and one oxygenated methyl [δ_H 4.11 t, $J_{(2', 1')}$ = 8.5 Hz, 2H, CH_2-OCO H-1’. The prodrug **2**'s detailed spectroscopic data is given in **Supporting Information S1**.

Prodrug 3: Hexadecyl 2-(2-((2,6-dichlorophenyl) amino) phenyl) acetate (3)

Similarly, the molecular formula $C_{30}H_{43}Cl_2NO_2$was determined from the EIMS of prodrug **3** and the HREI-MS, which revealed M+ at *m/z* 519.2671 with Δ ppm -0.6 and suggested a decreased double bond value of 9 (Calculated Molecular Weight (MW) 519.2661). Sharp bands may be seen in the IR spectrum at 3296 cm^{-1} (NH) and 2926.5-2854.1 cm^{-1} (aliphatic carbons). Moreover, a robust band at 1713.5 cm^{-1} (COOR). The compound's ^{1}H, and ^{13}C NMR chemical shifts revealed characteristic peaks for 30 carbons, including 16 aliphatic carbons, one methyl carbon [δ_H 0.9 (t) $J_{(15', 16')}$ = 8.8Hz H-16'], and one oxygenated methyl [δ_H 4.11 t, $J_{(2', 1'))}$ = 8.5Hz, 2H, CH_2-OCO H-1']= 8.5Hz, 2H, CH2-OCO H-1]. The prodrug **3**'s detailed spectroscopic data is given in **Supporting Information S1**.

Prodrug 4: Octadecyl 2-(2-((2,6-dichlorophenyl) amino) phenyl) acetate (4)

Likewise, the molecular formula $C_{32}H_{47}Cl_2NO_2$was determined from the EIMS of prodrug **4** and the HREI-MS, which revealed M+ at *m/z* 547.2984 with Δ ppm -1.4and suggested a decreased double bond value of 9 (Calculated Molecular Weight (MW) 547.2973). Sharp bands may be seen in the IR spectrum at 3397 cm^{-1} (NH) and 2921.4-2848.8 cm^{-1} (aliphatic carbons). Moreover, a robust band at 1715.1 cm^{-1} (COOR). The compound's ^{1}H, and ^{13}C NMR chemical shifts revealed characteristic peaks for 32 carbons, including 16 aliphatic carbons, one methyl carbon [δ_H 0.85 (t) $J_{(17', 18')}$ = 8.8Hz, H-18']and one oxygenated methyl [δ_H 4.11 t, $J_{(2', 1')}$ = 8.5Hz, 2H, CH_2-OCO H-1']. The prodrug **4** detailed spectroscopic data is given in **Supporting Information S1**.

Comparison of the IR data of Diclofenac with its prodrugs (1-4)

Diclofenac's FT-IR spectrum and the FT-IR spectrum of prodrugs (**1**-**4**) were contrasted (**Figure 1**). For all prodrugs, a shift from 1694.4 cm-1 to a higher vibration frequency value in the C=O stretching band is noticed when the drug's acid functionality was converted to an ester (1719 cm^{-1}, 1720.4 cm^{-1}, 1713.5 cm^{-1}, and 1713.5 cm^{-1} for prodrug 1, 2, 3, and 4, respectively). A stretching band in the region of 2919-2925 cm^{-1} is observed arising from the aliphatic chains that are connected to all prodrugs **1**-**4**, however this band is not present in DCF-I, indicating the absence of any aliphatic carbon chain. As shown in **Figure 1**, the production of ester prodrugs is confirmed by the presence of an aliphatic chain and a change in the values of the C=O stretching band.

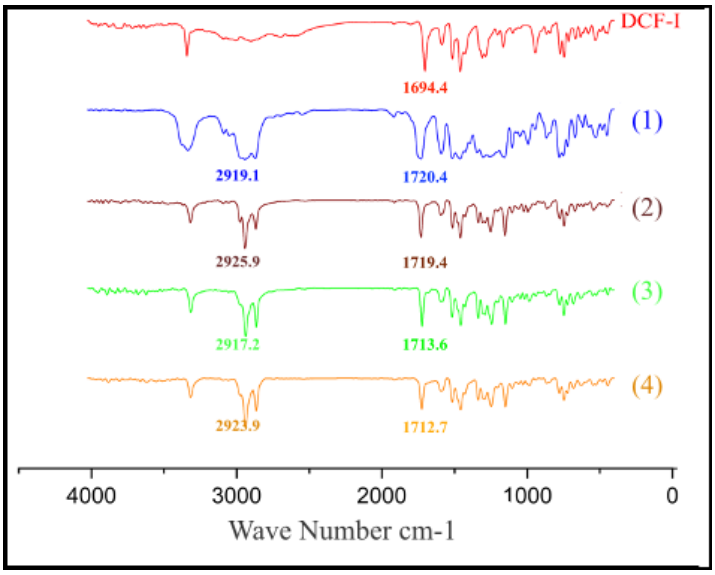

Figure-1: IR spectra of diclofenac drug (DCF-I) and synthesized prodrugs (**1**-**4**).

3.2. Prodrug nanoparticle Preparation and Characterization

Each prodrug was then formulated into nanoparticles as detailed above. As Diclofenac prodrug (**1**-**4**) do not form nanoparticles alone, DSPE-PEG_{2000}, an FDA approved drug excipient was used as stabilizer (Wang et al., 2012). Indeed, DSPE-PEG_{2000} is known to reduce crystallization and prevent Ostwald ripening (Doi et al., 1989). The strong hydrophobic interaction between prodrugs aliphatic chains and DSPE-PEG_{2000} aliphatic chains led to successful formulation of nanoparticles below 200 nm in size with a negative zeta potential, with no significant difference between the different prodrugs. All NP PdIs were below 0.2 proving their good monodispersity. These results show that the simple formulation process proposed for glucocorticoids can be extended to Diclofenac which possess different physico-chemical characteristics (Lorscheider et al., 2019b, 2019a). Nanoparticles were subjected to stability evaluation based on size, PdI, and zeta potential over time, as shown in **Figure 2**. All nanoparticles were stable for more than 30 days and exhibited hydrodynamic diameter of 110-150 nm. All nanoparticles have a negative surface charge between -29 and -49 mV. The polydispersity index (PdI) remains below 0.2 indicative of rather monodisperse nanoparticles. Only for prodrug **3** NPs maintained at room temperature a slight increase of the PdI was observed, a probable indication of aggregation but the PdI remained below 0.3 and we do not believe this is significant. Longer stability studies with microscopic observations would be needed. However, no obvious aggregation was observed over up to 35 days. These results are interesting as these formulations do not require purification or freeze-drying for medium-term storage before animal experiments. The aliphatic carbon chain present in prodrug structure most probably interacts with the distearyl chains of DSPE-PEG_{2000}, due to strong hydrophobic interactions, promoting the stability and absence of Ostwald ripening. In addition, the presence of hydrophilic PEG chains at the outer surface of NPs may also play a role in the stability of NPs through steric hindrance.

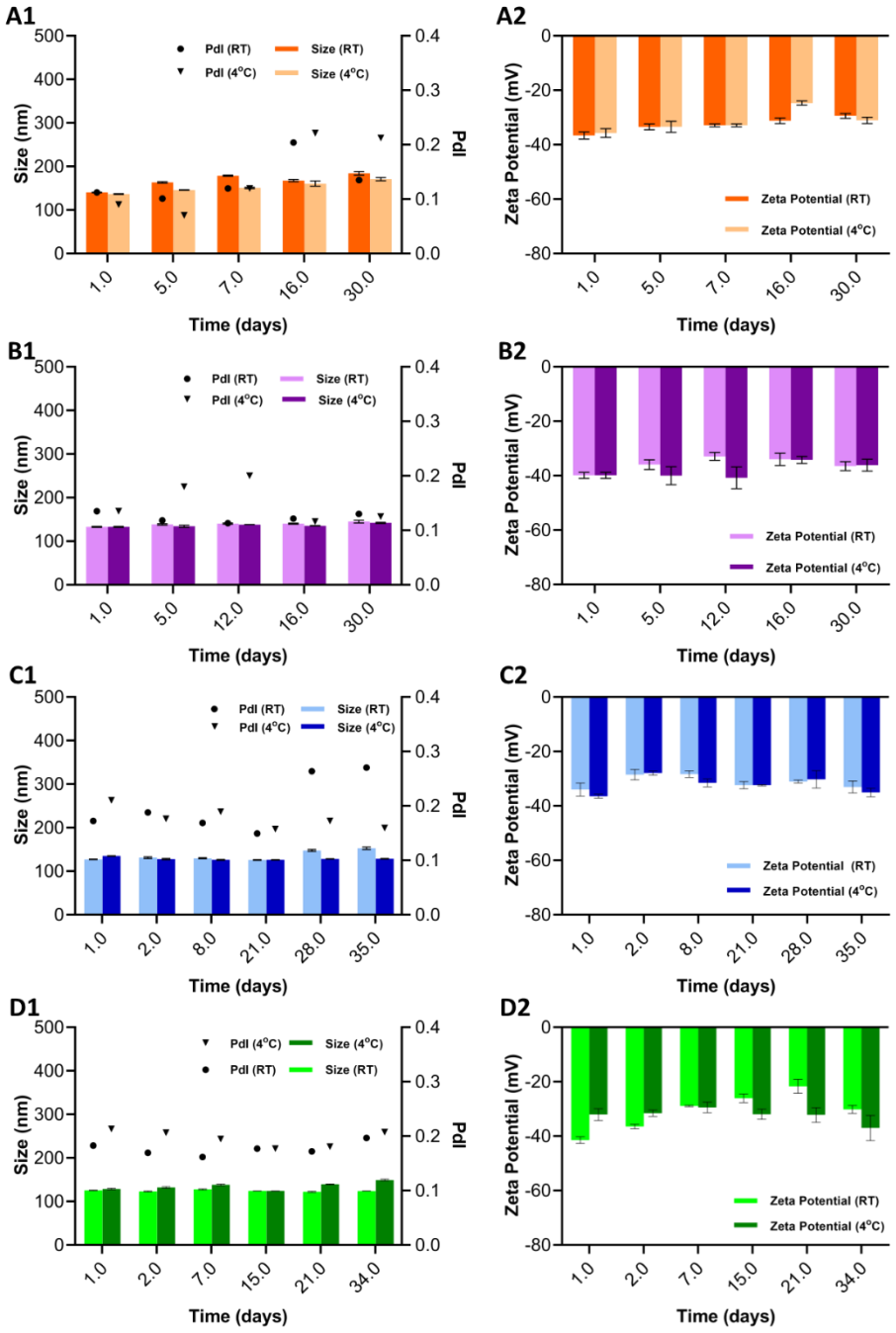

Figure-2: Nanoparticle size and PdI of Prodrug **1** NPs (A1), Prodrug **2** NPs (B1), Prodrug **3** NPs (C1) and Prodrug **4** NPs (D1) placed at 4 °C or room temperature (RT) overtime. Zeta potential of Prodrug **1** NPs (A2), Prodrug **2** NPs (B2), Prodrug **3** NPs (C2) and Prodrug **4** NPs (D2) placed at 4 °C or room temperature (RT) overtime.

3.3. Scanning Electron Microscopy (SEM) and Transmission Electron Microscopy (TEM) observations

SEM and TEM observations of the prepared nanoparticles were carried out (**Figure-3**). All nanoparticles, i.e., Prodrug (**1**-**4**) NPs showed homogeneity in size distribution of

nanoparticles and the sizes were in close agreement with values obtained from DLS technique, below 200 nm. No crystalline structure or aggregation was observed in the SEM/TEM images despite the drying occurring during sample preparation.

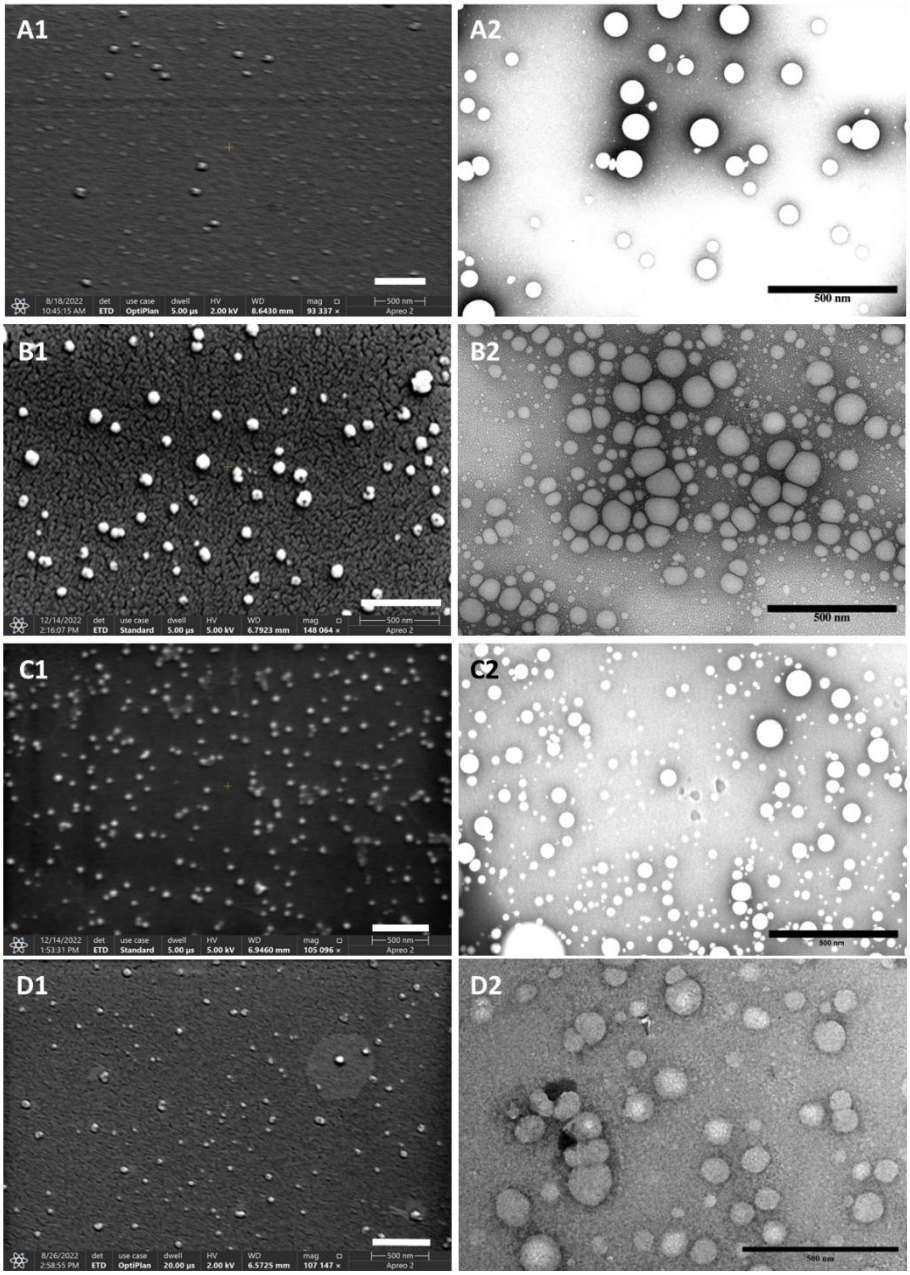

Figure-3: SEM micrographs of Prodrug **1** NPs (A1) Prodrug **2** NPs (B1), Prodrug **3** NPs (C1) and Prodrug **4** NPs (D1). TEM micrographs of Prodrug **1** NPs (A2) Prodrug **2** NPs (B2), Prodrug **3** NPs (C2) and Prodrug **4** NPs (D2) after negative staining. The scale bars represent 500 nm in each image.

3.4. Determination of encapsulation efficiency (EE) of prodrugs

Since DSPE-PEG_{2000} can form micelles (Kastantin et al., 2010), some prodrug could be solubilized in micelles and not only in nanoparticles. Encapsulation efficiency was determined by quantifying the amount of prodrugs in NPs by UPLC. After separation by ultracentrifugation, non-encapsulated prodrug in the supernatant was quantified, and their amount in NPs was calculated indirectly (**Figure 4**). All prodrug nanoparticles displayed very

high encapsulation efficiency from 90-91 % for C10 to C16 prodrugs up to 96 % for the more hydrophobic prodrug bearing a C18 aliphatic chain, namely prodrug **4** (Figure-4). These values are comparable with prodrug nanoparticles of glucocorticoids obtained by the same process (Pinheiro do Nascimento et al., 2022). The non-encapsulated prodrugs are probably solubilized within DSPE-PEG micelles (Kastantin et al., 2010). NP characterization suggests that the emulsion-evaporation method allows the production of small and stable NPs with high EE%.

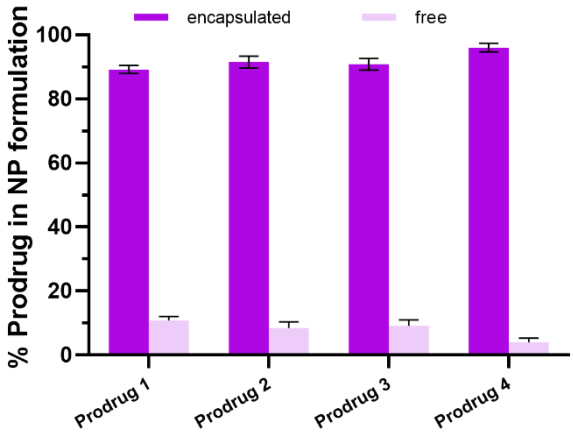

Figure-4: Encapsulation efficiency of prodrug in NPs **1**-**4**.

3.5. In vitro evaluation of prodrug NPs 1-4

3.5.1. Alamar Blue Assay

Alamar blue assay was performed to check the cytotoxicity of the diclofenac and prodrugs nanoparticles on THP-1 cell line. According to ISO guideline for the cell viability assay, potential cytotoxicity is defined as the cell viability decreases below 70% of the control. All Prodrug (**1**-**4**) NPs were safe and showed no toxicity for the tested concentration of 1, 10 and 100 µg/mL. Whereas, diclofenac sodium led to a IC_{50} of 20±2 µg/mL, below the higher concentration tested. All the prodrug NPs led to IC_{50} above 100 µg/mL. Therefore, the tested concentrations were screened in terms of TNF-α cytokine secretion inhibition except for diclofenac sodium which was only tested up to 10 µg/mL.

3.5.2. TNF-α cytokine secretion inhibition

To ensure that the anti-inflammatory activity of diclofenac was conserved after formulation, the release of the pro-inflammatory cytokines TNF- α by LPS-activated THP-1 cells in the cell culture medium was quantified after their exposure to prodrugs **1**-**4** NPs (**Figure-5**). The inhibition of TNF-α secretion appears to be dose dependent for both diclofenac sodium and prodrug nanoparticles, reaching from 80 to 100% inhibition for an equivalent diclofenac concentration of 100 µg/mL (**Figure-5**). Results confirm that prodrug formulation into NPs does not affect the therapeutic activity of the drug. Diclofenac is most probably released from prodrugs NPs due to the presence of esterases in the cell culture medium, and NPs can

therefore be tested *in vivo*. Prodrug **3** NPs were chosen for *in vivo* experiments as a representative formulation to compare them with dexamethasone prodrug nanoparticles bearing the same aliphatic chain length (Lorscheider et al., 2019b).

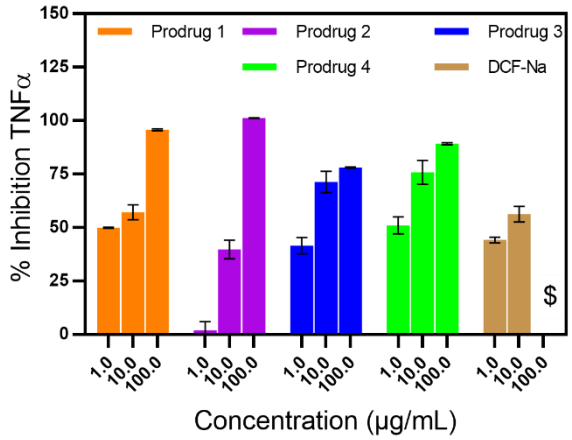

Figure-5: Inhibition of TNF-α secretion of LPS-activated THP1 cells incubated with Prodrug (1-4) NPs and diclofenac sodium at different equivalent concentrations diclofenac 1, 10 and 100 µg/mL for 24 h. The $ symbol indicates the 100 µg/mL concentration was not tested for diclofenac sodium due to toxicity.

3.6. Drug release studies from nanoparticles in murine plasma

To ensure diclofenac would be released in blood circulation once after injection of prodrug nanoparticles, Prodrug **3** NPs were incubated in murine plasma and diclofenac concentration quantified by UPLC as described above. Most likely due to hydrolysis by esterases present in plasma, we observed the release of diclofenac as soon as 30 minutes after the beginning of incubation with about 4% released (**Figure-6**). The concentration of the drug then increased up to 70% after 6 h of incubation. Afterwards the drug release reached a plateau probably because esterase concentration was not sufficient to degrade all prodrugs or because some prodrug remains protected from esterases in NPs or because diclofenac is degraded as it is released. This release profile is very similar to dexamethasone release in murine plasma observed with similar prodrug nanoparticles (Lorscheider et al., 2019b) or what is observed for diclofenac prodrug micelles incubated with porcine liver esterases (Assali et al., 2021).

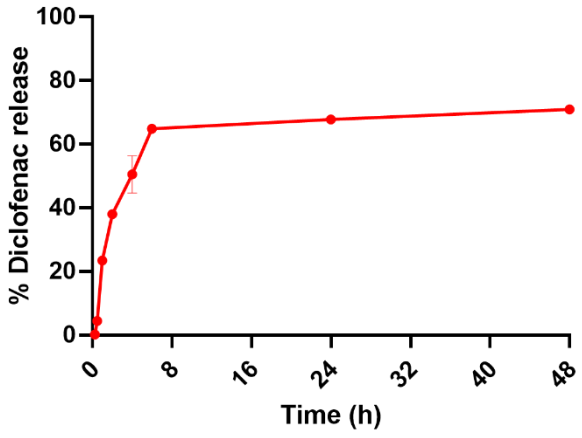

Figure-6: Diclofenac release profile in murine plasma from Prodrug **3** NPs upon incubation at 37°C.

3.7. *In Vivo* Studies on Collagen induced Arthritis murine model

Prodrugs **3** NPs were administered to mice as described above on days 31, 33 and 35 and compared with PBS or diclofenac sodium to assess the efficacy of the nanoparticulate formulation. Both the paw volume and the arthritic score were quantified and the data were analyzed using a two-way ANOVA followed by Dunnett multiple comparison tests (**Figure-7**). The activity of prodrug **3** NPs was evaluated by measuring the total arthritis score on all 4 paws for each mouse. Following the first injection, the paw volume of Prodrug **3** NPs group started to decrease although not significant compared to PBS or diclofenac sodium. The difference became significant (PBS vs NPs) in terms of paw volume only two days after the second injection. The 3rd injection did not lead to a further decrease and no significant difference could be observed. When considering the arthritic score, a score decrease became significant (PBS vs NPs) after the second injection also. One can conclude that Prodrug **3** NPs lead to a moderate decrease of inflammation as compared with PBS. When comparing with the soluble form of diclofenac the inflammation decrease is not significant. Increasing the number of animals or the dose schedule might improve result difference. However, although Prodrug **3** NPs were significantly more efficient than PBS, they induced a toxicity leading to half of mice dying after the 3rd injection. No signs of toxicity were observed for the soluble diclofenac group or PBS. After autopsy of the NPs group animals, the liver was found swollen and very black. Diclofenac hepatic toxicity is documented and is linked to mitochondrial injury (Nouri et al., 2017). Our hypothesis is the following: due to a modification of diclofenac biodistribution when administered as NPs versus a soluble form, NPs accumulated in the liver, leading to hepatic toxicity after third dose due to extensive accumulation. A full biodistribution study would be required to confirm this hypothesis. To promote the reduction of inflammation while avoiding hepatic toxicity using NPs would require to precisely study the No Observable Adverse Effect Level and the schedule of administration in the future.

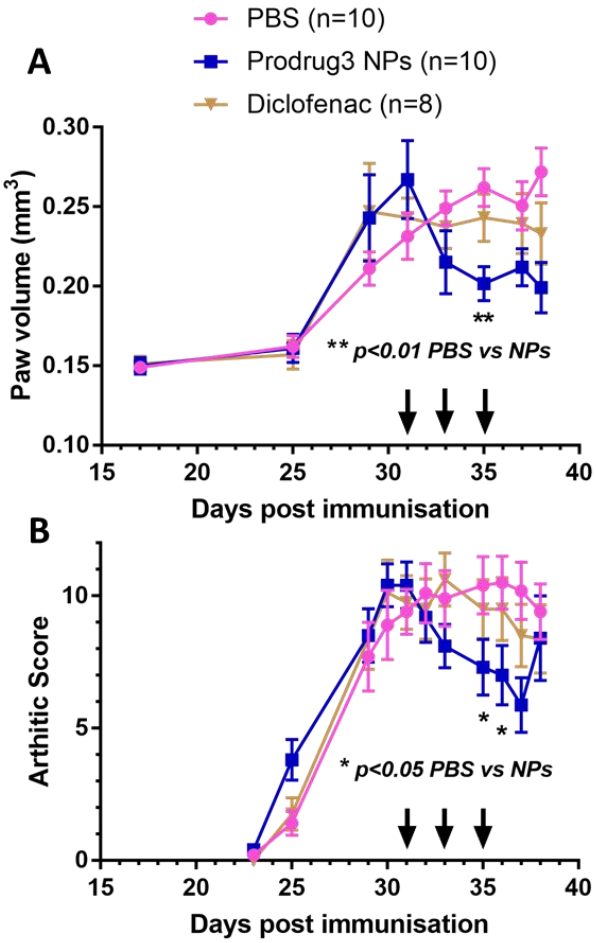

Figure-7: (A) Paw Volume and (B) Arthritic score of mice treated with PBS, Prodrug **3** NPs and Diclofenac as sodium salt. Statistical analysis was performed using 2way ANOVA and Dunnet post comparison tests.

4. Conclusion

We have successfully synthesized four lipidic prodrugs of Diclofenac by grafting C10, C12, C16 and C18 aliphatic chains through an ester bound. The prodrugs were easily formulated into NPs using DSPE-PEG_{2000} as the only excipient by an emulsion-evaporation process. Prodrugs NPs were spherical, small (110-150 nm), rather monodisperse and sterically stabilized by PEGylation. The formulation process allowed to obtain NPS with a prodrug encapsulation efficiency ranging from 91 to 96%. These results exhibit the potential of synthesizing lipidic prodrug of hydrophobic drugs to further formulate them into NPs using PEGylated lipids as excipients. NPs were considered suitable candidates for further *in vitro* & *in vivo* evaluation. NPs did not induce any toxicity on LPS-activated THP1 cells up to a concentration of 100 µg/mL (equivalent diclofenac) whereas diclofenac sodium salt IC_{50} was around 20 µg/mL. Following incubation of prodrug NPs with LPS-activated THP1 cells, a dose dependent inhibition of TNF-α was observed comparable to standard diclofenac sodium. Similarly, upon incubation in murine plasma, Prodrug **3** NPs most likely underwent an enzymatic cleavage and almost 70 % of diclofenac was released from nanoparticles in 8 hours. *In vivo* studies on a CIA murine model showed contrasted results: on one hand

Prodrug **3** NPs led to a significant decrease of arthritis score and of paw volume compared to PBS after the second injection, on the other hand the third injection induced an important hepatic toxicity with the death of half of the mice from the NPs group. To promote the reduction of inflammation while avoiding hepatic toxicity using NPs would require to precisely study the No Observable Adverse Effect Level and the schedule of administration in future studies.

Acknowledgments

The authors would like to acknowledge the organizers of Pakistan-France PERIDOT Research Mobility Program (No.PhaseVII-1/PERIDOT.R&D/HEC/2021), jointly implemented by the Higher Education Commission, Pakistan, and Ministry of Foreign Affairs & International Development (MAEDI) and the Ministry of Higher Education and Research (MESRI), France. The present work has benefited from the core facilities of Imagerie-Gif, (http://www.i2bc.paris-saclay.fr), member of IBiSA (http://www.ibisa.net), supported by "France-BioImaging" (ANR-10-INBS-04-01), and the Labex "Saclay Plant Science" (ANR-11-IDEX-0003-02).

References

Al-Amin, M.M., Uddin, M.M.N., Rahman, M.M., Reza, H.M., Rana, M.S., 2013. Effect of diclofenac and antidepressants on the inflammatory response in astrocyte cell culture. Inflammopharmacology 21, 421–425. https://doi.org/10.1007/S10787-013-0181-9

Al-Lawati, H., Vakili, M.R., Lavasanifar, A., Ahmed, S., Jamali, F., 2019. Delivery and Biodistribution of Traceable Polymeric Micellar Diclofenac in the Rat. J. Pharm. Sci. 108, 2698–2707. https://doi.org/10.1016/J.XPHS.2019.03.016

Alamanos, Y., Voulgari, P. V., Drosos, A.A., 2006. Incidence and prevalence of rheumatoid arthritis, based on the 1987 American College of Rheumatology criteria: a systematic review. Semin. Arthritis Rheum. 36, 182–188. https://doi.org/10.1016/J.SEMARTHRIT.2006.08.006

Andrianakos, A., Trontzas, P., Christoyannis, F., Kaskani, E., Nikolia, Z., Tavaniotou, E., Georgountzos, A., Krachtis, P., 2006. Prevalence and management of rheumatoid arthritis in the general population of Greece--the ESORDIG study. Rheumatology (Oxford). 45, 1549–1554. https://doi.org/10.1093/RHEUMATOLOGY/KEL140

Assali, M., Shawahna, R., Alhawareen, R., Najajreh, H., Rabaya, O., Faroun, M., Zyoud, A., Hilal, H., 2021. Self-assembly of diclofenac prodrug into nanomicelles for enhancing the anti-inflammatory activity. RSC Adv. 11, 22433–22438. https://doi.org/10.1039/d1ra03804d

Assali, M., Shawahna, R., Dayyeh, S., Shareef, M., Alhimony, I.A., 2018. Dexamethasone-diclofenac loaded polylactide nanoparticles: Preparation, release and anti-inflammatory activity. Eur. J. Pharm. Sci. 122, 179–184. https://doi.org/10.1016/j.ejps.2018.07.012

Carmona, L., Villaverde, V., Hernández-García, C., Ballina, J., Gabriel, R., Laffon, A., 2002. The prevalence of rheumatoid arthritis in the general population of Spain. Rheumatology (Oxford). 41, 88–95. https://doi.org/10.1093/RHEUMATOLOGY/41.1.88

Chatzidionysiou, K., Emamikia, S., Nam, J., Ramiro, S., Smolen, J., Van Der Heijde, D., Dougados, M., Bijlsma, J., Burmester, G., Scholte, M., Van Vollenhoven, R., Landewé, R., 2017. Efficacy of glucocorticoids, conventional and targeted synthetic disease-modifying antirheumatic drugs: a systematic literature review informing the 2016 update of the EULAR recommendations for the management of rheumatoid arthritis. Ann. Rheum. Dis. 76, 1102–1107. https://doi.org/10.1136/ANNRHEUMDIS-2016-210711

Doi, M., Ishida, T., Sugio, S., Imagawa, T., Inoue, M., 1989. Physicochemical properties of dexamethasone palmitate, a high fatty acid ester of an anti-inflammatory drug: Polymorphism and crystal structure. J. Pharm. Sci. 78, 417–422. https://doi.org/10.1002/jps.2600780515

Dolati, S., Sadreddini, S., Rostamzadeh, D., Ahmadi, M., Jadidi-Niaragh, F., Yousefi, M., 2016. Utilization of nanoparticle technology in rheumatoid arthritis treatment. Biomed. Pharmacother. 80, 30–41. https://doi.org/10.1016/J.BIOPHA.2016.03.004

Gaudin, A., Yemisci, M., Eroglu, H., Lepetre-Mouelhi, S., Turkoglu, O.F., Donmez-Demir, B., Caban, S., Sargon, M.F., Garcia-Argote, S., Pieters, G., Loreau, O., Rousseau, B., Tagit, O., Hildebrandt, N., Le Dantec, Y., Mougin, J., Valetti, S., Chacun, H., Nicolas, V., Desmaele, D., Andrieux, K., Capan, Y., Dalkara, T., Couvreur, P., 2014. Squalenoyl adenosine nanoparticles provide neuroprotection after stroke and spinal cord injury. Nat Nanotechnol 9, 1054–1062. https://doi.org/10.1038/nnano.2014.274

Jacobs, P., Bissonnette, R., Guenther, L.C., 2011. Socioeconomic burden of immune-mediated inflammatory diseases--focusing on work productivity and disability. J. Rheumatol. Suppl. 88, 55–61. https://doi.org/10.3899/JRHEUM.110901

Kastantin, M., Missirlis, D., Black, M., Ananthanarayanan, B., Peters, D., Tirrell, M., 2010. Thermodynamic and kinetic stability of DSPE-PEG(2000) micelles in the presence of bovine serum albumin. J. Phys. Chem. B 114, 12632–12640. https://doi.org/10.1021/JP1001786

Langley, P.C., Mu, R., Wu, M., Dong, P., Tang, B., 2011. The impact of rheumatoid arthritis on the burden of disease in urban China. J. Med. Econ. 14, 709–719. https://doi.org/10.3111/13696998.2011.611201

Leng, D., Chen, H., Li, G., Guo, M., Zhu, Z., Xu, L., Wang, Y., 2014. Development and comparison of intramuscularly long-acting paliperidone palmitate nanosuspensions with different particle size. Int. J. Pharm. 472, 380–385. https://doi.org/10.1016/j.ijpharm.2014.05.052

Lorscheider, M., Tsapis, N., Simón-Vázquez, R., Guiblin, N., Ghermani, N., Reynaud, F., Canioni, R., Abreu, S., Chaminade, P., Fattal, E., 2019a. Nanoscale Lipophilic Prodrugs of Dexamethasone with Enhanced Pharmacokinetics. Mol. Pharm. 16, 2999–3010. https://doi.org/10.1021/acs.molpharmaceut.9b00237

Lorscheider, M., Tsapis, N., Ur-Rehman, M., Gaudin, F., Stolfa, I., Abreu, S., Mura, S., Chaminade, P., Espeli, M., Fattal, E., Mujeeb-ur-Rehman, Gaudin, F., Stolfa, I., Abreu, S., Mura, S., Chaminade, P., Espeli, M., Fattal, E., 2019b. Dexamethasone palmitate nanoparticles: An efficient treatment for rheumatoid arthritis. J. Control. Release 296, 179–189. https://doi.org/10.1016/J.JCONREL.2019.01.015

Maksimenko, A., Dosio, F., Mougin, J., Ferrero, A., Wack, S., Reddy, L.H., Weyn, A.-A., Lepeltier, E., Bourgaux, C., Stella, B., Cattel, L., Couvreur, P., 2014. A unique squalenoylated and nonpegylated doxorubicin nanomedicine with systemic long-circulating properties and anticancer activity. Proc. Natl. Acad. Sci. U. S. A. 111, E217-26. https://doi.org/10.1073/pnas.1313459110

Mellado, M., Martínez-Muñoz, L., Cascio, G., Lucas, P., Pablos, J.L., Rodríguez-Frade, J.M., 2015. T Cell Migration in Rheumatoid Arthritis. Front. Immunol. 6. https://doi.org/10.3389/FIMMU.2015.00384

Myasoedova, E., Davis, J., Matteson, E.L., Crowson, C.S., 2020. Is the epidemiology of rheumatoid arthritis changing? Results from a population-based incidence study, 1985-2014. Ann. Rheum. Dis. 79, 440–444. https://doi.org/10.1136/ANNRHEUMDIS-2019-216694

Neovius, M., Simard, J.F., Askling, J., 2011. Nationwide prevalence of rheumatoid arthritis and penetration of disease-modifying drugs in Sweden. Ann. Rheum. Dis. 70, 624–629. https://doi.org/10.1136/ARD.2010.133371

Nouri, A., Heidarian, E., Nikoukar, M., 2017. Effects of N-acetyl cysteine on oxidative stress and TNF-α gene expression in diclofenac-induced hepatotoxicity in rats. Toxicol. Mech. Methods 27, 561–567. https://doi.org/10.1080/15376516.2017.1334732

Ozbakir, B., Crielaard, B.J., Metselaar, J.M., Storm, G., Lammers, T., 2014. Liposomal corticosteroids for the treatment of inflammatory disorders and cancer. J. Control. Release 190, 624–636.

https://doi.org/10.1016/J.JCONREL.2014.05.039
Pinheiro do Nascimento, L., Tsapis, N., Reynaud, F., Desmaële, D., Moine, L., Vergnaud, J., Abreu, S., Chaminade, P., Fattal, E., 2022. Mannosylation of budesonide palmitate nanoprodrugs for improved macrophage targeting. Eur. J. Pharm. Biopharm. 170, 112–120. https://doi.org/10.1016/J.EJPB.2021.12.001
Quan, L., Zhang, Y., Crielaard, B.J., Dusad, A., Lele, S.M., Rijcken, C.J.F., Metselaar, J.M., Kostková, H., Etrych, T., Ulbrich, K., Kiessling, F., Mikuls, T.R., Hennink, W.E., Storm, G., Lammers, T., Wang, D., 2014. Nanomedicines for inflammatory arthritis: head-to-head comparison of glucocorticoid-containing polymers, micelles, and liposomes. ACS Nano 8, 458–466. https://doi.org/10.1021/nn4048205
Tsakos, M., Schaffert, E.S., Clement, L.L., Villadsen, N.L., Poulsen, T.B., 2015. Ester coupling reactions--an enduring challenge in the chemical synthesis of bioactive natural products. Nat. Prod. Rep. 32, 605–632. https://doi.org/10.1039/C4NP00106K
Wang, R., Xiao, R., Zeng, Z., Xu, L., Wang, J., 2012. Application of poly(ethylene glycol)-distearoylphosphatidylethanolamine (PEG-DSPE) block copolymers and their derivatives as nanomaterials in drug delivery. Int. J. Nanomedicine 7, 4185–4198. https://doi.org/10.2147/IJN.S34489